RECOGNITION TECHNOLOGY OF AGRICULTURAL PICKING ROBOT BASED ON IMAGE DETECTION TECHNOLOGY
/
基于图像检测技术的农业采摘机器人识别技术

Yujie Jin [1]

School of Information Science and Engineering, Changsha Normal University, Changsha, Hunan, 410199 / China
Tel: 13006254198; E-mail: uggzqp@163.com

ABSTRACT

As a kind of intelligent agricultural equipment, picking robots are of great significance for improving the efficiency of agricultural production. However, the main bottleneck restricting the development of picking robots today is the positioning and control in image recognition. Therefore, an agricultural picking control method based on visual servo technology is proposed. This method can accurately control the picking hand of the picking robot on the basis of building an eye-hand relationship model and an online identification system. With the tomato picking process as the background, the effectiveness of the method was verified. The test results of image feature points show that there is a small error between the stable feature points and the expected image feature points. In addition, the image plane trajectory of the picking robot is relatively smooth, and there is no vibration or overshoot. In addition, from its density distribution characteristics, it can be seen that the picking hand movement is a continuous acceleration stage at the beginning of the control, and at the end of the control, the characteristic points gradually tend to the desired characteristics, and the output of the control system is relatively stable. It can be seen from this that the model has better control performance. This method has certain practical significance for the improvement of agricultural picking efficiency.

摘要

采摘机器人作为一种智能农业设备，对提高农业生产效率具有重要意义。然而，目前制约采摘机器人发展的主要瓶颈是图像识别中的定位与控制。为此，提出了一种基于视觉伺服技术的农业采摘控制方法。该方法在建立眼-手关系模型和在线辨识系统的基础上，能够准确地控制采摘机器人的拣手。以番茄采摘过程为背景，验证了该方法的有效性。图像特征点测试结果表明，采摘机器人的稳定特征点与期望的图像特征点之间仅存在误差。另外，拾取机器人的像面轨迹比较平滑，没有振动和过冲现象。另外，从其密度分布特征可以看出，采摘手的运动在控制开始时是一个连续的加速阶段，在控制结束时，特征点逐渐趋向于期望的特性，控制系统的输出相对稳定。由此可见，该模型具有较好的控制性能。该方法对提高农业采摘效率具有一定的现实意义。

INTRODUCTION

Agriculture industry is an important guarantee for food security in all countries in the world. Agricultural robots are widely used in agricultural production to improve the ability of agricultural robots to sense their work and precise control, which can not only improve agricultural modernization level, but also improve international status in agricultural production and technology exchange. Among them, the fruit and vegetable picking robot, as a key field of agricultural science and technology research, is of great significance to agricultural modernization. However, today's fruit and vegetable picking robots usually have poor picking results due to positioning errors and motion errors *(Bao, Cai and Qi, 2016)*. In order to overcome the problem of low control accuracy of fruit and vegetable picking operations in complex environments, the article explores the control error of fruit and vegetable picking robots, and proposes a micro-control method of fruit and vegetable picking robots based on visual servo technology to effectively improve agricultural picking efficiency.

The micro-control of the picking robot achieves precise positioning in a small space by installing a monocular camera on the robot arm to adjust the image error *(Bargoti et al, 2017)*. Its core lies in setting the control purpose of the robot, so as to automatically obtain image information and analyse it, and output the feedback information of the machine control in a short time to achieve a good effect on the control of the robot trajectory *(Mehta et al, 2016)*.

---

[1] *Yujie Jin, As. PhD. Eng.*

According to the observable features on the plane and the texture target plane, a suitable control law is derived, and the estimated factors of unknown constant force disturbance are introduced into the control law, and then the effectiveness of the controller is proved through experiments. *(Wang S. et al., 2018).* In order to study the visual servo control of space-based space robots, *Dong G.* and his colleagues conducted an in-depth discussion on non-cooperative target pose and motion estimation algorithms. Finally, experiments prove the applicability of the control scheme *(Dong et al., 2015).* In order to effectively solve the problem of visual servo control for robots without degrees of freedom, the *Tsai C.Y.* research team proposed a new hybrid switched reactive visual servo control structure, which is derived from perception and reaction behaviour and does not require inverse interaction matrix calculations *(Tsai et al., 2015).* This control structure helps to simplify the realization process of the visual servo system and improve the control efficiency *(Serra et al., 2016).* *Szymon Krupínski et al.* proposed a visual servo control method for underwater robots based on non-linear inertial auxiliary images. This method uses the homomorphic matrix between two images of a plane scene as feedback information to control the system in a cascaded manner in the control design. The development of dynamics is more robust to the uncertainty and perturbation of the model than the traditional solution that only considers the traditional solution of system kinematics. *(Szymon Krupínski et al., 2017).* The research team of Silveira G discussed the problem of vision-based robot control and proposed a new strength-based non-metric visual servo technology. This technology does not consider the target characteristics of the observation object, the displacement of the camera and the relative attitude, and can achieve the dynamic decoupling of the translation control error. Finally, through corresponding experiments, the effectiveness of the technology is proved. *(Silveira et al., 2020).*

Combined with experiments to verify the effector, the results show that the effector has great potential in promoting kiwifruit harvest. The research team outlined the research and development activities of agricultural robots in recent years, and discussed some specific issues related to the precise control of weeds and fertilizer applications by robots. *(Wang J, Zhou G and Wei X., 2019).* With the development of picking robots, Tao Y and his colleagues proposed an apple automatic recognition method based on point cloud data in order to improve the robot's recognition ability and perception ability in three-dimensional space. *(Tao Y., Zhou J., 2017).* The research team introduced an intelligent machine that helps farmers pick lemons. The machine is a mechanical arm that can cut lemons from trees. This machine can help farmers complete their work effortlessly, greatly reducing labour *(Yan H.J., Bai G. and He J.Q., 2010).* In order to manage the precise application of fertilization and water in agriculture, *Zavala-Yoe R et al.* constructed an agricultural intelligent production model. The original model is equipped with a laser sensor, which can measure the content of water, fertilizer or any other nutrients in the crops. This is of great significance for improving the level of agricultural modernization. *(Zavala-Yoe R. et al., 2017).*

MATERIALS AND METHODS
Eye-hand relationship model building

The essence of robot visual servoing is the problem of nonlinear system control, which is generally described by the eye-hand relationship model. *(Qingqing S., Bin W., Jiawei Y., Yizhi L. and Tongming Y., 2020)* Therefore, the first task of constructing an agricultural picking robot model based on visual servo technology should be to establish an eye-hand relationship model, and then use an online identification system to set its real-time status, and finally establish a control strategy design plan, so the agricultural based on visual servo technology is obtained. *(Changbin H, Yong Y, Decheng W, Hongjian W. and Bingnan Y., 2020).* According to the positional relationship between the camera and the mechanical structure, the eye-hand configuration of the agricultural picking robot can be divided into an eye-on-hand configuration and an eye-fixed configuration. The two configurations are shown in fig.1.

The eye-fixed configuration refers to fixing the camera on a certain working scene of the agricultural picking system to ensure that the entire picking process is captured and it is convenient to integrate the image information into the visual control system. The image obtained by the eye-fixed configuration is clearer and the image resolution is higher. *(Min J, Chunguang W, and Pengpeng W., 2020)* The eye-on-hand configuration refers to fixing the camera on the moving arm of the agricultural picking robot so that the camera and the moving arm are synchronized. The main advantage is that the posture of the robot arm can be flexibly adjusted to minimize the distance between the camera and the target object, so as to ensure the accuracy of picking the target, and at the same time improve the image observation accuracy. Because the eye-on-hand configuration is more conducive to the precise positioning of the target picking object, this time the eye-on-

hand configuration is mainly used. In the process of building the relationship model, the most important thing is to define the coordinate relationship.
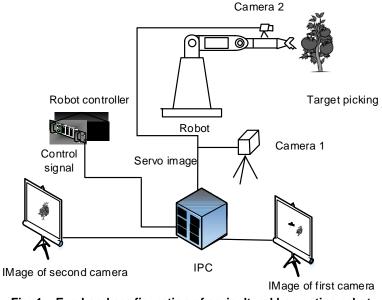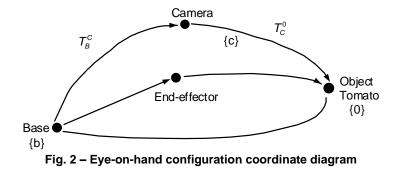

Fig. 1 – Eye-hand configuration of agricultural harvesting robot

This study uses the relationship structure shown in Figure 2 as the determination rule.

Fig. 2 – Eye-on-hand configuration coordinate diagram

Taking the plane centre of gravity of the target pick as the target $^bp_a=[\ ^bp_x,\ ^bp_y,\ ^bp_z]^T$, and the spatial coordinate of the target pick under the camera coordinate system $\{C\}$ is $^cp_a=[\ ^cp_x,\ ^cp_y,\ ^cp_z]^T$, ^cP_z represents the depth information of the target pick, and the optical axis of the camera is integrated with the Z_c axis. In addition, the unit distance pixels in each direction on the image plane $\{i\}$ are assumed, respectively denoted by N_x, N_y, the plane coordinates of the centre of the image plane are represented by (u_0, V_0), and the pixel coordinates of the target plane after image processing are represented by $f=[u,v]^T$, which is obtained by formula (1) The projected coordinate of the target image is $^ip=[x, y]^T$, and the formula (1) is shown below.

$$\begin{cases} x = (u - u_0)\,/\,N_x \\ y = (v - v_0)\,/\,N_y \end{cases} \tag{1}$$

The plane coordinates of the target picking object obtained by the projection principle and the projection coordinates are converted according to the corresponding calculation model. The conversion principle is as follows.

$$\begin{cases} x = \lambda \cdot \dfrac{^cp_x}{^cp_z} \\[2mm] y = \lambda \cdot \dfrac{^cp_y}{^cp_z} \end{cases} \tag{2}$$

λ in the above formula represents the focal length of the camera. Differentiating the formula (2) gives the results shown below.

$$\begin{cases} \dot{x} = -\lambda \cdot \dfrac{{}^c\dot{p}_x \cdot {}^c p_z - {}^c p_x \cdot {}^c \dot{p}_z}{\left({}^c p_z\right)^2} \\[4mm] \dot{y} = -\lambda \cdot \dfrac{{}^c\dot{p}_y \cdot {}^c p_z - {}^c p_y \cdot {}^c \dot{p}_z}{\left({}^c p_z\right)^2} \end{cases} \tag{3}$$

The above formula is written in matrix form, and the result is shown in formula (3). Formula (3) shows that there is a nonlinear relationship between the transformation of the plane coordinate position of the target picking and the transformation of the spatial coordinate position.

$$\begin{bmatrix} \dot{x} \\ \dot{y} \end{bmatrix} = \lambda \begin{bmatrix} \dfrac{1}{{}^c p_z} & 0 & -\dfrac{{}^c p_x}{\left({}^c p_z\right)^2} \\[4mm] 0 & \dfrac{1}{{}^c p_z} & -\dfrac{{}^c p_y}{\left({}^c p_z\right)^2} \end{bmatrix} \tag{4}$$

For the principle of coordinate conversion in each coordinate system, see formula (5). ${}^cP_a$ in formula (5) represents the position vector of the origin of the camera coordinate system, and ${}^c_bR$ represents the relative position of the two coordinate systems.

$$ {}^c p_a = {}^c_b R \cdot \left({}^b p_a - {}^b p_c \right) \tag{5}$$

Differentiating formula (5) yields the results shown below.

$$ {}^c \dot{p}_a = {}^c_b \dot{R} \cdot \left({}^b p_a - {}^b p_c \right) + {}^c_b R \cdot \left({}^b \dot{p}_a - {}^b \dot{p}_c \right) \tag{6}$$

${}^bP_a$ in the above formula represents the coordinate translation speed of the target picking relative to the agricultural picking robot, and ${}^bP_c$ represents the coordinate translation speed of the camera relative to the agricultural picking robot. Because the target picking is usually at rest, it is assumed that the translation speed is 0, that is, ${}^bP_a=0$, and the formula (6) is rewritten using the relevant calculation model. The results are as follows.

$$ {}^c \dot{p}_a = {}^c_b \dot{R} \cdot \left({}^b p_a - {}^b p_c \right) - {}^c_b R \cdot \dot{p}_c \tag{7}$$

The camera follows the robot arm to make a rotary motion ${}^c\Omega=({}^cw_x,\ {}^cw_y,\ {}^cw_z)$ and a translation motion ${}^cT=({}^cT_x,\ {}^cT_y,\ {}^cT_z)$, and the calculation results shown below are obtained.

$$ {}^c \dot{p}_a = \begin{bmatrix} {}^c\dot{p}_x \\ {}^c\dot{p}_y \\ {}^c\dot{p}_z \end{bmatrix} = \begin{bmatrix} -1 & 0 & 0 & 0 & -{}^c p_z & {}^c p_y \\ 0 & -1 & 0 & {}^c p_z & 0 & -{}^c p_x \\ 0 & 0 & -1 & -{}^c p_y & {}^c p_x & 0 \end{bmatrix} \begin{bmatrix} {}^cT_x \\ {}^cT_y \\ {}^cT_z \\ {}^cW_x \\ {}^cW_y \\ {}^cW_z \end{bmatrix} \tag{8}$$

The two formulas (4) and (8) are integrated, and the results are shown in formula (9). Formula (9) shows that there is a close correlation between the change in the image plane of the target picking and the change in camera position. That is, the image Jacobian matrix as shown in (10).

$$ J_{image} = \begin{bmatrix} -\dfrac{\lambda}{{}^c p_z} & 0 & \dfrac{x}{{}^c p_z} & \dfrac{xy}{\lambda} & -\dfrac{\lambda^2 + x^2}{\lambda^2} & y \\[4mm] 0 & -\dfrac{\lambda}{{}^c p_z} & \dfrac{y}{{}^c p_z} & \dfrac{\lambda^2 + y^2}{\lambda} & -\dfrac{xy}{\lambda} & -x \end{bmatrix} \tag{9}$$

The above formula is the conventional analytical formula of the image Jacobian matrix. The image Jacobian matrix is closely related to the image plane position and the target picking depth. The monocular camera cannot accurately measure the depth of the target picks, so it is necessary to use the image Jacobian matrix to convert the plane information and the base coordinate information of the target picks to overcome the depth measurement difficulty.

Online identification design

In the process of using visual servo technology for micro-control, if the estimated value of the image Jacobian matrix cannot be corrected online, then the performance of the image feedback system cannot be controlled. In severe cases, the visual system will cause a greater degree of Shock. Existing image Jacobian matrix estimation methods usually introduce tentative motion, which will affect the operation of the visual servo system. In addition, there is a lot of noise interference in the image information processing link, and the identification algorithm should be able to have high robustness to effectively deal with the image processing link noise and avoid the degradation of matrix estimation performance. The online identification algorithm should not be too cumbersome, and the processing time should be reduced as much as possible. So as to effectively improve the response efficiency of the system. Based on the above analysis, this study uses Kalman filter to complete the online identification of the image Jacobian matrix. The founder of Kalman filter estimation method is Kalman. He proposed the algorithm in 1960. The core idea is to estimate the minimum state value of error variance. The spatial model of the linear discrete system of Kalman filter is shown below.

$$\begin{cases} x(k) = Ax(k) + \eta(k) \\ z(k) = Cx(k) + v(k) \end{cases} \tag{10}$$

There are $Z \in R^m$, $X \in R$ in the above formula, and these two represent the state vector and output vector of the visual system, respectively, η, v is the noise vector, and A, C represents the state equation coefficient matrix. In order to improve the efficiency of the linear discrete system state assessment, the corresponding prerequisites need to be set.

$$E(\eta(k)) = 0, \mathrm{cov}\{\eta(k), \eta(j)\} = R_\eta \delta_{kj}$$
$$E(v(k)) = 0, \mathrm{cov}\{v(k), v(j)\} = R_v \delta_{kj}$$
$$\mathrm{cov}\{\eta(k), v(j)\} = R_{\eta v} = 0, \forall k, j \tag{11}$$
$$Z_k = (z(1)\ z(2)......z(k))$$

The Kalman filter estimation method can be used to evaluate the state of the visual system by using relevant expressions (Formulas (12)-(15)).

$$Q(k+1) = AP(k) + R_\eta \tag{12}$$

$$K(k+1) = Q(k+1)C^T \left[CQ(K+1)C^T + R_v \right]^{-1} \tag{13}$$

$$P(k+1) = \left[I - K(k+1)C \right] Q(K+1) \tag{14}$$

$$\hat{x}(k+1) = A\hat{x}(k) + K(k+1)\left[z(k+1) - CA\hat{x}(k) \right] \tag{15}$$

Based on the image Jacobian matrix of the eye-on-hand relationship model, the relevant definitions in the application of agricultural picking machines are as follows, where q represents the robot's hand n order vector, and f represents the current picking robot through the visual sensor, then the feature vector of m-dimensional image is obtained.

$$\dot{f} = J(q) \cdot \dot{q} \tag{16}$$

The above formula is discretized, and the result is shown in the following formula.

$$f(k+1) = f(k) + J(q(k)) \cdot \Delta q(k) \tag{17}$$

The Kalman filter is used to complete the online identification of the Jacobian matrix of the image, that is, the process of accurately estimating all the elements in $J(q(k))$, and the mn×1-dimensional observation vector shown below is constructed.

$$x = \left(\frac{\partial f_1}{\partial q}\ \frac{\partial f_2}{\partial q}\ ....\ \frac{\partial f_m}{\partial q} \right)^T \tag{18}$$

The vector of the image Jacobian matrix $J(q)$ in row i is represented by $\frac{\partial f_i}{\partial q} = \left(\frac{\partial f_i}{\partial q_1}\ \frac{\partial f_i}{\partial q_2}\ ....\ \frac{f_i}{\partial q_n} \right)$ $(i-1,2,...,m)$ in the above formula. The state value of the visual system is defined by the observation vector of the image Jacobian matrix. The movement of the robot arm will cause the system output to change with the change of the image characteristics. That is, there is a corresponding linear relationship $y(k)=f(k+1)-f(k)$ between the two, and the state equation shown below is obtained.

$$\begin{cases} x(k+1) = x(k) + \eta(k) \\ y(k) = C(k) \cdot x(k) + v(k) \end{cases} \tag{19}$$

The state noise vector and the image observation noise are respectively represented by $\eta(k)$, $v(k)$ in the above formula, and $C(k)$ represents the diagonal matrix. For the corresponding expression form, see the following formula.

$$C(k) = \begin{pmatrix} \Delta q(k)^T & \cdots & 0 \\ \vdots & \ddots & \vdots \\ 0 & \cdots & \Delta q(k)^T \end{pmatrix}_{m \times n} \tag{20}$$

According to the Kalman filter estimation principle shown in (12)-(15), a recursive estimation model of the image Jacobian matrix is established.

$$\begin{cases} Q(k+1) = P(k) + R_\eta \\ K(k+1) = Q(k+1) \times C^T(k) \cdot \left[C(k) \cdot Q(k+1) \cdot C^T(k) + R_v \right]^{-1} \\ P(k+1) = \left[I - K(k+1) \cdot C(k) \right] \cdot Q(k+1) \\ \hat{x}(k+1) = \hat{x}(k) + K(k+1) \cdot \left[y(k+1) - C(k) \cdot \hat{x}(k) \right] \end{cases} \tag{21}$$

In the above formula, R_n, R_V represents the noise variance matrix, and $P(K)$ represents the state estimation error variance matrix. The corresponding initial value can be set to $P(o)$ and expressed by the unit matrix I_{m*n}. The initial value of state estimation can be calculated by least square method. When the hand of the agricultural picking robot is located at the initial position, the estimated value of the Jacobian matrix of the image can be obtained by calculating the estimated value of the Jacobian matrix of the image according to the trial motion Δq_1, Δq_2 and the observation model. (Eq.22).

$$\hat{J}(0) = \left(\Delta f_1 \ \Delta f_2 \right) \cdot \left(\Delta q_1 \ \Delta q_2 \right)^{-1} \tag{22}$$

In order to avoid the tentative motion behaviour of agricultural picking robots, before iterative calculation of the image Jacobian matrix, the depth value needs to be estimated according to the image plane size of the picking target. Because the image Jacobian matrix will be continuously updated by iteration, this is a process of continuous convergence of depth estimation until the required requirements are met.

Visual servo control design

According to the form of visual feedback signals, agricultural picking robots can be divided into position-based visual servos and image-based visual servos. The position-based visual servo can estimate the position of the target by judging the image information of the target. This kind of estimation error is small and has high applicability. Image-based visual servos can feedback control visual information by judging the characteristics of target images. There is no need to estimate the position of the target. In the case where the eye-on-hand configuration is selected, the image-based visual servo control system is shown in fig. 3, the control amount is calculated according to the image feature error, and the robot's motion space is adjusted using the relevant transformation model to promote the machine. The arm approaches the picking target. When the difference between the image feature and the actual feature is small, it can be considered that the agricultural picking robot has a high visual servo accuracy.
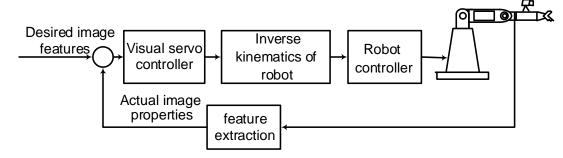

Fig. 3 - Visual servo control structure of agricultural picking robot based on image

According to the related performance of vision system of agricultural picking robot, PID control design is adopted to serve the controller vision. As the most typical controller design method, PID control is applied to the robot visual servo system with high frequency. This kind of control method can realize the arbitrary space representation of the error. The robot is controlled mainly through the Cartesian space instruction. The robot can build an appropriate PID controller based on the error information obtained by feedback. The construction model is shown below.

$$u(k) = K_p e(k) + K_I \sum_{i=1}^{k} e(k) + K_D \left(e(k) - e(k-1) \right) \tag{23}$$

In the above formula, $U(k)$ represents the machine control input, while $K_D,\ K_p\ K_k$ represents the integral coefficient matrix, proportional and differential coefficient matrix, and $e(k)$ represents the error display signal. In order to achieve the visual feedback effect of the eye-on-hand, the visual servo control must meet the requirement that the image features of the target picking material continue to approach the position of the image plane. Therefore, the image error $e(t)$ is defined as a systematic error, and is handled by referring to the following formula.

$$e(t) = f^d - f(t) \tag{24}$$

f^l in the above formula represents the image feature of the target picking, and there is $f_d=(u_c, v_c)^T$, which represents the position of the image plane. In addition, the control amount of the robot is defined, and the definition formula is as follows.

$$u(k) = \Delta q(k+1) = q(k+1) - q(k) \tag{25}$$

In order to ensure the micro-control effect, it is necessary to eliminate the system static error, and process the image processing noise. Using the PI control strategy, the visual servo control expression of the agricultural picking robot is obtained, see formula (14).

$$u(k+1) = J - 1 \cdot \left(c_1 e(k) + c_2 \sum_{i=0}^{k} e(i) \right) \tag{26}$$

$C_1\ C_2$ in the above formula respectively corresponds to the control ratio and integral processing coefficient of the PI controller. The visual servo control process of agricultural picking is shown in the following figure. The control process includes a total of six steps, which are the desired position of the target picking, visual servo control processing, the robot acquiring the target picking image, the visual servo system processing image, and the image Jacobian. The matrix estimates that these six steps cooperate with each other to complete the picking of agricultural products.
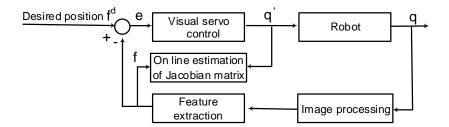

Fig. 4 - Visual servo control flow of agricultural picking robot image

RESULTS
Experiment design and preparation

In order to verify the effectiveness of the micro-control model of the agricultural picking robot constructed above, this experiment used tomatoes as the picking object. For the design of the experimental platform, see fig. 5. Before the experiment starts, the picking robot needs to be moved near the tomatoes to be picked. The right arm is set as an air suction picker to fix the target picking object. The waist coordinate system of the picking robot is set to the world coordinate system. The monocular camera is installed on the lower right side of the air-suction picking robot, and the two axes of the monocular camera coincide with the two axes of the cutting hand. The installation requirements of the monocular camera can ensure that the target picks appear in the image plane. The image plane of the monocular camera is set to $650{\times}450$ pixel, the feature point is set to the image centre of the target picking object, and it is recorded as p, and the corresponding image plane

coordinate is marked as *(u,v)*. The u axis is used as the main direction of movement of the shearing grip along the X axis, and the v axis is used as the main direction of movement of the shearing grip along the Z axis. These two axes respectively control the translation direction of the shearing grip. Due to the influence of the R type cutting hand's own attributes, the incision range of the target pick into the type R cutting hand cannot be accurately calculated, so it is necessary to use the teaching method to obtain the actual position of the target pick. It is generally believed that when the centre point of the target tomato is within the standard range *(250,270)* or *[190,210]*, the cutting position of the picker is more accurate.
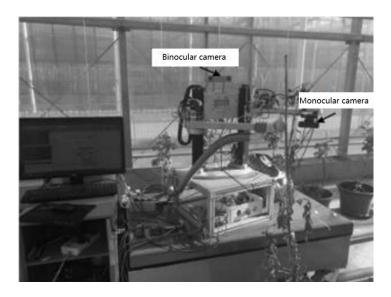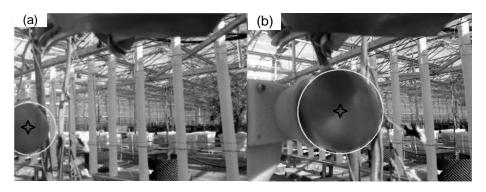

Fig. 5 - Visual servo test platform of agricultural harvesting robot

Analysis of results

After completing the installation of the experimental instrument and parameter settings, the above model is officially applied, and the application results are shown in Figure 6. It can be seen from fig.6 that the initial feature plane coordinate of the target picking is *(42, 148)*, the final stable feature plane coordinate is *(263,198)*, and the error from the expected image feature point is *(3,-4)*. It can be seen from this that the model has high accuracy for the image recognition of the picking target position.
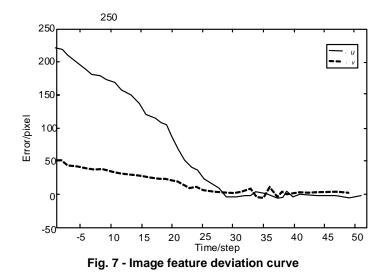

(a) Initial position   (b) Final position

Fig. 6 - Image position comparison of target picking

In addition, the image characteristic deviation curve of the visual servo control system is obtained by the above method, as shown in fig. 7. It can be seen from fig. 7 that compared with the desired image feature points, the feature points at the final stable state are slightly lower, and there is a deviation of about 4 pixels between the two. Therefore, it can be considered that the visual servo micro-control model can meet the requirements of tomato picking.

Fig. 7 - Image feature deviation curve

The movement path of the feature points of the target picking on the image plane can be seen in Fig. 8. It can be seen from fig. 8 that the movement trajectory of the image plane is relatively smooth and no significant vibrations and overshoots are found. It can be seen that the design of the visual servo micro-control model is more scientific and reasonable. When the feature point is close to the desired feature point, the speed of picking the hand gradually slows down, and the deceleration process will continue until the feature point enters the allowable control range. The movement path of the plane image of the feature point is more tortuous and is not the optimal route, but this is also the characteristic of visual servo control.

CONCLUSIONS

In order to improve the efficiency of agricultural picking and solve the problems of positioning error and motion error during the picking process, this paper builds a micro-control model of agricultural picking robot based on visual servo technology. After the completion of the experimental platform construction and parameter settings, the validity of the model was verified. The experimental results show that the initial feature plane coordinates of the target picks are *(42,128)*, and the final stable feature plane coordinates are (263.198). Compared with the expected image feature points, the error is only *(3,-4)*. In addition, according to the movement trajectory of the target picking object, the image plane movement trajectory of the picking robot generally looks smooth, without obvious vibration or overshoot, and it can be judged that the design of the visual servo micro-control model is reasonable. The characteristics of its density distribution indicate that the picking hand movement is higher in the initial stage of control and continues to increase. When the feature points gradually tend to the desired feature, the image error will decrease and the output of the control system will stabilize. In summary, the model can adapt to the complex environment of agricultural picking and effectively overcome binocular positioning errors and motion errors. Although this model can provide a method reference for the research of agricultural picking robot identification technology, there are still problems in the experiment that the simulation of picking times is small and the accuracy of the experiment is not high enough.

ACKNOWLEDGEMENTS

REFERENCES

[1]   Bao G, Cai S, Qi L., (2016), Multi-template matching algorithm for cucumber recognition in natural environment. *Computers & Electronics in Agriculture,* Issue 127, pp.754-762, England;

[2]   Bargoti S, Underwood J P., (2017), Image Segmentation for Fruit Detection and Yield Estimation in Apple Orchards. *Journal of Field Robotics*, Vol.34, Issue 6, pp.1039-1060, USA;

[3]   Changbin H, Yong Y, Decheng W, Hongjian W, Bingnan Y., (2020), An experimental investigation of soil layer coupling failure characteristics on natural grassland by passive subsoiler- type openers. *INMATEH-Agricultural Engineering*, Vol.61, Issue 2, pp. 49-58, Romania;

[4]   Dong G, Zhu Z H., (2015), Position-based visual servo control of autonomous robotic manipulators. *Acta astronautica,* Issue 115, pp.291-302, England;

[5]   Mehta S, Burks T F., (2016), Adaptive Visual Servo Control of Robotic Harvesting Systems. *Ifac Papersonline,* Vol.49, Issue 16, pp.287-292, Netherlands;

[6]   Min J, Chunguang W, Pengpeng W., (2020), CFD Numerical simulation of temperature and airflow distribution in pigsty based on grid independence verification. *INMATEH-Agricultural Engineering*, Vol.61, Issue 2, pp. 241-250, Romania;

[7]   Qingqing S, Bin W, Jiawei Y, Yizhi L, Tongming Y., (2020), An omni-directional electric pruning saw for forest tending. *INMATEH-Agricultural Engineering*, Vol.61, Issue 2, pp. 35-40, Romania;

[8]   Serra P, Cunha R, Hamel T., (2016), Landing of a Quadrotor on a Moving Target Using Dynamic Image-Based Visual Servo Control. *IEEE Transactions on Robotics,* Vol.32, Issue 6, pp.1524-1535, USA;

[9]   Silveira G, Mirisola L, Morin P., (2020), Decoupled Intensity-Based Nonmetric Visual Servo Control. *IEEE Transactions on Control Systems Technology,* Vol.28, Issue 2, pp.566-573, USA;

[10]   Szymon Krupínski, Allibert G, Hua M D., (2017), An Inertial-Aided Homography-Based Visual Servo Control Approach for (Almost) Fully Actuated Autonomous Underwater Vehicles. *IEEE Transactions on Robotics,* Vol.33, Issue 5, pp.1041-1060, USA;

[11]   Tao Y, Zhou J., (2017), Automatic apple recognition based on the fusion of colour and 3D feature for robotic fruit picking. *Computers & electronics in agriculture,* Issue 142, pp.388-396, England;

[12]   Tsai C Y, Wong C C, Yu C J., (2015), A Hybrid Switched Reactive-Based Visual Servo Control of 5-DOF Robot Manipulators for Pick-and-Place Tasks. *Systems Journal, IEEE,* Vol.9, Issue 1, pp.119-130, USA;

[13]   Wang J, Zhou G, Wei X., (2019), Experimental characterization of multi-nozzle atomization interference for dust reduction between hydraulic supports at a fully mechanized coal mining face. *Environmental Science and Pollution Research*, Vol.26, Issue 10, pp.10023-10036, Germany;

[14]   Wang S, He X, Song J., Wang et al., (2018), Effects of xanthan gum on atomization and deposition characteristics in water and Silwet 408 aqueous solution. *International Journal of Agricultural and Biological Engineering*, Vol.11, Issue 3, pp.29-34, China;

[15]   Yan H J, Bai G, He J Q., (2010), Model of droplet dynamics and evaporation for sprinkler irrigation. *Biosystems Engineering*, Vol.106, Issue 4, pp.440-447, USA;

[16]   Zavala-Yoe R, Ramirez-Mendoza R A, Silverio García-Lara., (2017), A 3-SPS-1S Parallel Robot-based Laser Sensing for Applications in Precision Agriculture SCI-Journal. *Soft Computing,* Issue 21, pp.641-650, USA;